Modern Problems of Acoustics and Hydroacoustics

Modern Problems of Acoustics and Hydroacoustics

Edited by

Alexander Kleshchev

Cambridge Scholars Publishing

Modern Problems of Acoustics and Hydroacoustics

Edited by Alexander Kleshchev

This book first published 2022

Cambridge Scholars Publishing

Lady Stephenson Library, Newcastle upon Tyne, NE6 2PA, UK

British Library Cataloguing in Publication Data
A catalogue record for this book is available from the British Library

ISBN (10): 1-5275-8670-7
ISBN (13): 978-1-5275-8670-3

CONTENTS

PREFACE

This collection is called “Modern problems of acoustics and hydroacoustics” and covers a wide range of theoretical and applied issues in the areas: isotropic and anisotropic scatterers and waveguides; hydroacoustic antennas for the echo sounder; frequency, pulse and transitional characteristics of the electrodynamic loudspeaker; the application of correlation effects in technical acoustics; and numerical solutions of sound scattering problems by bodies of non-analytical forms using the boundary element method.

The authors are grateful to V. Yu. Chizhov and F. F. Legusha for their helpful comments on the research results.

Authors would also like to thank V. I. Gromova, S. G. Evstatiev, M. S. Il’menkova, B. P. Ivanov, M. A. Kleshchev, S. M. Kleshchev, A. S. Klimenkov, Yu. A. Klokov, E. I. Kuznetsova, M. Moshchuk, M. M. Pavlov, and the CSP team, including Helen Edwards, Rebecca Gladders, Clementine Joly, Joanne Parsons, Sophie Edminson, Mhairi Nicol, and Adam Rummens, for editing, proofreading, and publishing of our collection.

CHAPTER ONE

ISOTROPIC AND ANISOTROPIC SCATTERERS AND WAVEGUIDES

A. A. KLESHCHEV

1.1. Characteristics of Isotropic Spheroidal Scatterers

In this section, the resonances of prolate and oblate spheroidal bodies (in their entirety and in the form of shells), which are impacted by three-dimensional and axisymmetric angles of irradiation, are going to be investigated. Debye's potentials have been used to calculate the three-dimensional pattern of irradiation in order to solve the diffraction problem. Various publications are devoted to the resonances of elastic spheroidal bodies [1, 2 – 9]. Debye first proposed expanding the vector potential $\vec{A}$ and the scalar potentials U and V in his publication [10], which is devoted to studying the behavior of light waves near the local point or line. Later, this approach was used to solve the diffraction problems in the electromagnetic wave diffraction of a sphere, a circular disk, and a paraboloid revolution [11 – 16], as well as for the diffraction by spheroidal bodies in longitudinal and transverse waves [1, 17].

When Debye's potentials are applied to problems based on the theory of dynamic elasticity, it occurs as follows: the displacement vector $\vec{u}$ of an elastic isotropic medium obeys the Lame equation

$$(\lambda+\mu) graddiv\vec{u} - \mu curlcurl\vec{u} = -\rho\omega^2\vec{u}, \qquad (1.1)$$

where λ and μ are Lame constants, ρ is the density of the isotropic medium, and ω is the circular frequency of harmonic vibrations.

According to the Helmholtz theorem, the displacement vector $\vec{u}$ is expressed through scalar Φ and vector $\vec{\Psi}$ potentials as follows:

$$\vec{u} = -grad\Phi + curl\vec{\Psi} \tag{1.2}$$

Substituting equation (1.2) in equation (1.1), we obtain two Helmholtz equations, which include one scalar equation for Φ and one vector equation for $\vec{\Psi}$:

$$\Delta\Phi + h^2\Phi = 0, \tag{1.3}$$

$$\Delta\vec{\Psi} + k_2^2\vec{\Psi} = 0. \tag{1.4}$$

Here $h = \omega / c_1$ is the wavenumber of the longitudinal elastic wave; c_1 is the velocity of this wave; $k_2 = \omega / c_2$ is the wavenumber of the transverse elastic wave; and c_2 is the velocity of the transverse wave. In the three-dimensional case, the variables involved in scalar equation (1.3) can be separated into 11 coordinate systems. As for equation (1.4), in the three-dimensional problem, it yields three independent equations for each of components of the vector function $\vec{\Psi}$ in the Cartesian coordinate system alone. To overcome this difficulty, one can use Debye's potentials U and V , that obey the Helmholtz scalar equation as follows:

$$\Delta V + k_2^2 V = 0; \;\; \Delta U + k_2^2 U = 0. \tag{1.5}$$

The vector potential $\vec{\Psi}$ (according to Debye) is expanded in potentials V and U as follows:

$$\vec{\Psi} = curlcurl(\vec{R}U) + ik_2 curl(\vec{R}V) \tag{1.6}$$

where $\vec{R}$ is the radius vector of a point of the elastic body or the elastic medium.

Let us demonstrate the efficiency of using Debye's potentials to solve the three-dimensional diffraction problems in the acoustical diffraction of an elastic spheroidal shell. The advantage of the representation (1.6) becomes evident, if we consider that potentials V and U obey the Helmholtz scalar equation. It is convenient to represent components of $\vec{\Psi}$ in the spherical coordinate system by expressing them through U, V, and $\vec{R}$ and then, using vector analysis formulas, to change to spheroidal components. The expressions for spherical components of the vector function $\vec{\Psi}(\Psi_R, \Psi_\theta, \Psi_\varphi)$ in terms of Debye's potentials take the following form [1]:

$$\Psi_R = (\partial\xi/\partial R)^2(\partial^2 B/\partial\xi^2) + 2(\partial\xi/\partial R)(\partial\eta/\partial R)(\partial^2 B/\partial\xi\partial\eta) + (\partial\eta/\partial R)^2(\partial^2 B/\partial\eta^2) +$$

$$(\partial^2\xi/\partial R^2)(\partial B/\partial\xi) + (\partial^2\eta/\partial R^2)(\partial B/\partial\eta) + k_2^2 B, \qquad (1.7)$$

$$\Psi_\theta = [h_0(\xi^2 - 1 + \eta^2)]^{-1}[(\partial\xi/\partial\theta)(\partial\xi/\partial R)(\partial^2 B/\partial\xi^2) + (\partial\xi/\partial\theta)(\partial\eta/\partial R)(\partial^2 B/\partial\xi\partial\eta) +$$

$$(\partial\xi/\partial R)(\partial\eta/\partial\theta)(\partial^2 B/\partial\xi\partial\eta) + (\partial\eta/\partial R)(\partial\eta/\partial\theta)(\partial^2 B/\partial\eta^2) + (\partial B/\partial\xi)(\partial^2\xi/\partial R\partial\theta) +$$

$$(\partial B/\partial\eta)(\partial^2\eta/\partial R\partial\theta)] + ik_2(\sin\theta)^{-1}(\partial V/\partial\varphi), \qquad (1.8)$$

$$\Psi_\varphi = [h_0(\xi^2 - 1 + \eta^2)^{1/2}\sin\theta]^{-1}[\partial\xi/\partial R)(\partial^2 B/\partial\xi\partial\varphi) + (\partial\eta/\partial R)(\partial^2 B/\partial\eta\partial\varphi) - ik_2 \times$$

$$[(\partial\xi/\partial\theta)(\partial V/\partial\xi) + (\partial\eta/\partial\theta)(\partial V/\partial\eta)], \qquad (1.9)$$

$$B = h_0(\xi^2 - 1 + \eta^2)^{1/2}U; -1 \le \eta \le +1; 1 \le \xi \le +\infty.$$

Spheroidal components of the function $\vec{\Psi}(\Psi_\xi, \Psi_\eta, \Psi_\varphi)$ are expressed as follows [1]:

$$\Psi_\xi = \Psi_R(h_0/h_\xi)\xi(\xi^2 - 1 + \eta^2)^{-1/2} + \Psi_\theta(h_0/h_\xi)(\xi^2 - 1 + \eta^2)^{1/2}(\partial\theta/\partial\xi), \quad (1.10)$$

$$\Psi_\eta = \Psi_R(h_0/h_\eta)\eta(\xi^2 - 1 + \eta^2)^{-1/2} + \Psi_\theta(h_0/h_\eta)(\xi^2 - 1 + \eta^2)^{1/2}(\partial\theta/\partial\eta), \quad (1.11)$$

$$\Psi_{\varphi} \equiv \Psi_{\varphi}, \tag{1.12}$$

$$h_{\xi} = h_0(\xi^2 - \eta^2)^{1/2}(\xi^2 - 1)^{1/2}; \; h_{\eta} = (\xi^2 - \eta^2)^{1/2}(1 - \eta^2)^{1/2}.$$

Let us consider a scatterer in the form of an isotropic elastic spheroidal shell (Fig. 1-1). All potentials, including the plane wave potential Φ_0, the scattered wave potential Φ_1, the scalar shell potential Φ_2, Debye'spotentials U and V, and the potential Φ_3 of the gas filling the shell can be expanded in spheroidal functions:

$$\Phi_0 = 2\sum_{m=0}^{\infty}\sum_{n\geq m}^{\infty} i^{-n}\varepsilon_m \overline{S}_{m,n}(C_1,\eta_0)\overline{S}_{m,n}(C_1,\eta)R_{m,n}^{(1)}(C_1,\xi)\cos m\varphi, \tag{1.13}$$

$$\Phi_1 = 2\sum_{m=0}^{\infty}\sum_{n\geq m}^{\infty} B_{m,n}\overline{S}_{m,n}(C_1,\eta)R_{m,n}^{(3)}(C_1,\xi)\cos m\varphi; \tag{1.14}$$

$$\Phi_2 = 2\sum_{m=0}^{\infty}\sum_{n\geq m}^{\infty}[C_{m,n}R_{m,n}^{(1)}(C_l,\xi) + D_{m,n}R_{m,n}^{(2)}(C_l,\xi)]\overline{S}_{m,n}(C_l,\xi)\cos m\varphi; \tag{1.15}$$

$$\Phi_3 = 2\sum_{m=0}^{\infty}\sum_{n\geq m}^{\infty} E_{m,n}R_{m,n}^{(1)}(C_2,\xi)\overline{S}_{m,n}(C_2,\eta)\cos m\varphi; \tag{1.16}$$

$$U = 2\sum_{m=1}^{\infty}\sum_{n\geq m}^{\infty}[F_{m,n}R_{m,n}^{(1)}(C_t,\xi) + G_{m,n}R_{m,n}^{(2)}(C_t,\xi)]\overline{S}_{m,n}(C_t,\eta)\sin m\varphi; \tag{1.17}$$

$$V = 2\sum_{m=0}^{\infty}\sum_{n\geq m}^{\infty}[H_{m,n}R_{m,n}^{(1)}(C_t,\xi) + I_{m,n}R_{m,n}^{(2)}(C_t,\xi)]\overline{S}_{m,n}(C_t,\eta)\cos m\varphi, \tag{1.18}$$

$\overline{S}_{m,n}(C_1,\eta)$ represents the angular spheroidal function; $R_{m,n}^{(1)}(C_1,\xi)$, $R_{m,n}^{(2)}(C_1,\xi)$, and $R_{m,n}^{(3)}(C_1,\xi)$ represent the radial spheroidal functions of the first, second, and third kinds $C_l = hh_0$; $C_t = k_2h_0$; $C_1 = kh_0$, k is the wavenumber of the sound wave in the liquid; $C_2 = k_1h_0$, k_1 is the wavenumber of the sound wave in the gas filling the shell; h_0 represents the half-focal distance; $B_{m,n}, C_{m,n}, D_{m,n}, E_{m,n}, F_{m,n}, G_{m,n}, H_{m,n}$ and $I_{m,n}$ are unknown expansion coefficients.

The expansion coefficients are determined from the physical boundary conditions presented at two surfaces of the shell (ξ_0 and ξ_1; see Fig. 1-1) [1]:

(i) The continuity of the normal displacement component at both of the boundaries ξ_0 and ξ_1;

(ii) The normal stress on the outside boundary of the elastic shell is equal to the sound pressure in the liquid (ξ_0) and the normal stress on the inner boundary of the shell is equal to the sound pressure in the gas (ξ_1);

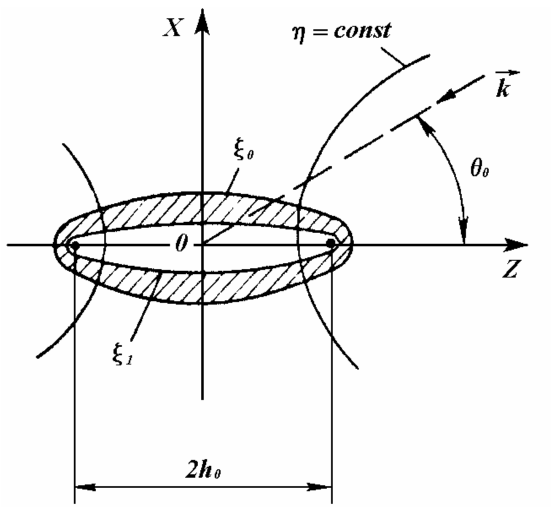

Figure 1-1: The elastic spheroidal shell in a harmonic plane wave field

(iii) The absence of tangential stresses at both shell boundaries, ξ_0 and ξ_1.

The corresponding expressions for boundary conditions take the following form [1]:

$$(h_\xi)^{-1}(\partial/\partial\xi)(\Phi_0+\Phi_1)=(h_\xi)^{-1}(\partial\Phi_2/\partial\xi)+(h_\eta h_\varphi)^{-1}[(\partial/\partial\eta)(h_\varphi\Psi_\varphi)-(\partial/\partial\varphi)(h_\eta\Psi_\eta)]_{\xi=\xi_0}; \quad (1.19)$$

$$(h_\xi)^{-1}(\partial\Phi_1/\partial\xi)=(h_\xi)^{-1}(\partial\Phi_2/\partial\xi)+(h_\eta h_\varphi)^{-1}[(\partial/\partial\eta)(h_\varphi\Psi_\varphi)-(\partial/\partial\varphi)(h_\eta\Psi_\eta)]_{\xi=\xi_1}; \quad (1.20)$$

$$-\lambda_0 k^2(\Phi_0+\Phi_1)=-\lambda h^2\Phi_2+2\mu[(h_\xi h_\eta)^{-1}(\partial h_\xi/\partial\eta)u_\eta+(h_\xi)^{-1}(\partial u_\xi/\partial\xi)]_{\xi=\xi_0}; \quad (1.21)$$

$$-\lambda_1 k_1^2\Phi_3=-\lambda h^2\Phi_2+2\mu[(h_\xi h_\eta)^{-1}(\partial h_\xi/\partial\eta)u_\eta+(h_\xi)^{-1}(\partial u_\xi/\partial\xi)]_{\xi=\xi_1}; \quad (1.22)$$

$$0=(h_\eta/h_\xi)(\partial/\partial\xi)(u_\eta/h_\eta)+(h_\xi/h_\eta)(\partial/\partial\eta)(u_\xi/h_\xi)_{\xi=\xi_0;\xi=\xi_1}; \quad (1.23)$$

$$0=(h_\varphi/h_\xi)(\partial/\partial\xi)(u_\varphi/h_\varphi)+(h_\xi/h_\varphi)(\partial/\partial\varphi)(u_\xi/h_\xi)_{\xi=\xi_0;\xi=\xi_1}, \quad (1.24)$$

where $h_\varphi=h_0(\xi^2-1)^{1/2}(1-\eta^2)^{1/2}$; λ_0 is the bulk compression coefficient of the liquid and λ_1 is the bulk compression coefficient of the gas filling the shell,

$$u_\xi=(h_\xi)^{-1}(\partial\Phi_2/\partial\xi)+(h_\eta h_\varphi)^{-1}[(\partial/\partial\eta)(h_\varphi\Psi_\varphi)-(\partial/\partial\varphi)(h_\eta\Psi_\eta)];$$
$$u_\eta=(h_\eta)^{-1}(\partial\Phi_2/\partial\eta)+(h_\xi h_\varphi)^{-1}[(\partial/\partial\varphi)(h_\xi\Psi_\xi)-(\partial/\partial\xi)(h_\varphi\Psi_\varphi)];$$
$$u_\varphi=(h_\varphi)^{-1}(\partial\Phi_2/\partial\varphi)+(h_\xi h_\eta)^{-1}[(\partial/\partial\xi)(h_\eta\Psi_\eta)-(\partial/\partial\eta)(h_\xi\Psi_\xi)].$$

The substitution of series (1.13)–(1.18) in boundary conditions (1.19)–(1.24) yields an infinite system of equations to determine the desired coefficients. Due to the orthogonality of the trigonometric functions, $\sin m\varphi$ and $\cos m\varphi$, the infinite system of equations breaks into infinite subsystems with fixed numbers, m. Each of the subsystems is solved usingthe truncation method. The number of retained terms of expansions (1.13)–(1.18) is increased with a greater wave size for the given potential.

The solution to the axisymmetric problem of sound waves diffraction from elastic spheroidal bodies was presented in [2, 3], and [1, 8, 9].

The characteristics of the prolate gas-filled shell were calculated for two angles of irradiation: $\theta_0 = 0^0$ and $\theta_0 = 90^0$. In a different scale, Figure 1-2 shows the modules of the angular characteristics of the $|D(\theta)|$ scattering of a steel prolate gas-filled spheroidal shell (curve 1), a soft prolate spheroid (curve 2), and a hard spheroid (curve 3) impacted by the sound wave at an angle of $\theta_0 = 0^0$, where $C_1 = 1,0$.

Figures 1-3 and 1-4 present the same angular distributions, but C_1 is the wave size; $C_1 = 3,1$ (for the elastic shell), $C_1 = 3,0$ (for the ideal spheroid), and $C_1 = 10,0$ (for the ideal spheroid). The notations of the curves for all three figures are identical. An analysis of the results shows that for an angle of $\theta_0 = 0^0$ and a wave dimension of $C_1 = 1,0$ (see Fig. 1-2), the angular characteristic of the elastic shell is equal to the characteristic of the hard spheroid. When $C_1 = 3,1$ and the irradiation angle of the impact is equal to $\theta_0 = 0^0$, the situation becomes indeterminate. The angular characteristic of the shell has a dipole character at the hard spheroid (see Fig.1-3). In parallel with the increase of the wave dimension C_1, the character of the sound scattering from the shell remains complicated (see Fig. 1-4). In the lit region, the characteristic is $|D(\theta)|$ in the hard spheroid but, in the shaded region, it is nearer to the shade lobe of the soft spheroid than the shadow lobe of a hard spheroid. From known angular characteristics of $D(\theta,\varphi)$ it is possible to calculate relative backscattering of the cross-sections (σ_0) from the elastic spheroidal bodies can be calculated [1]. Figure 1-5 shows the mathematical term for the relative backscattering of cross-sections σ_0 of prolate spheroids with a semi axes correlation of 1:10 $(\xi_0 = 1,005)$, which are impacted by the sound wave at an axially symmetric angle of irradiation $(\theta_0 = 0^0)$. The behavior of the solid elastic spheroid is very similar to that of the ideal hard scatterer. This is seen through a comparison of the angular characteristics $D(\theta,\varphi)$ in steel and ideal spheroids. This is a coincidence and can be observed everywhere, with the exception of the resonance point, $C = 7,4$. This resonance is called a Rayleigh surface wave [1, 30, 34, 36]. At a wave dimension of $C =$ 7,4, the surface contour of the continuous steel prolate spheroid is 2,5 λ_R, where λ_R is the length of a Rayleigh-type wave. The velocity of the wave c_R is equal to 2889 m/s; however, on the planar boundary of the steel-vacuum, the velocity of the Rayleigh wave is equal to 2980 m/s.

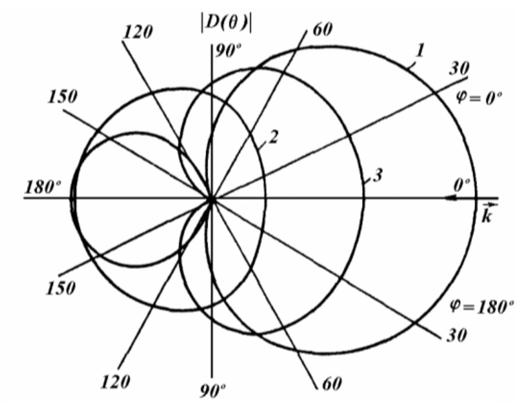

Figure 1-2: Modules of angular characteristics for spheroidal scatterers

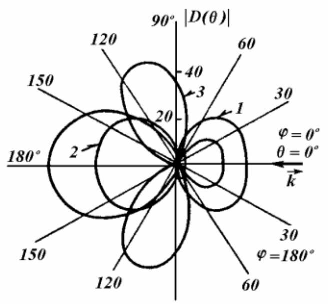

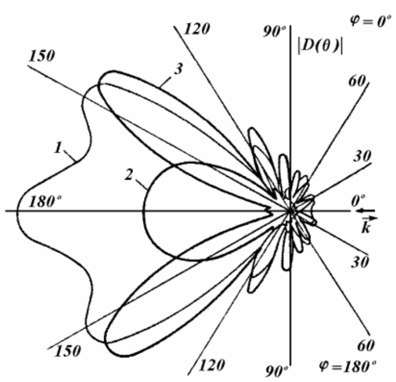

Figure 1-3: Modules of the angular characteristics of spheroidal scatterers
Figure 1-4: Modules of the angular characteristics of spheroidal scatterers

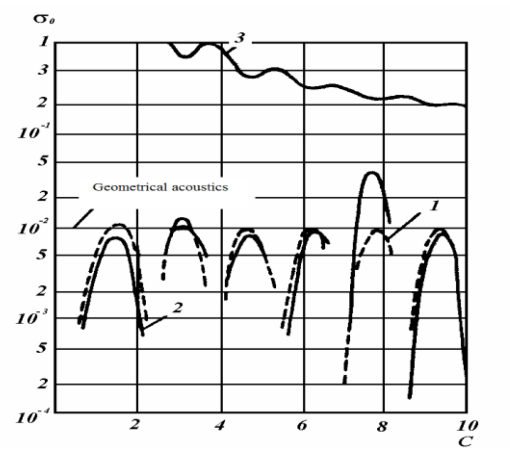

Figure 1-5: The relative backscattering of prolate spheroid cross-sections

Figure 1-6 shows the relative backscattering in the cross-sections σ_0 of oblate spheroids with a semi-axes correlation of 1:10 $(\xi_0 = 0,1005)$ when the notations coincide with Figure 1-5 otations through an axially symmetric angle of irradiation $\theta_0 = 0^0$.

This will occur until the rthe notationesonance of the zeroth antisymmetrical- flexural wave $(C \approx 5,3)$ σ_0 of the steel oblate spheroidis closer to the σ_0 of the soft spheroid, whereas for $C > 5,3$, it approaches the σ_0 of the hard spheroid, although the angular characteristic $D(\theta)$ obtained for the elastic spheroid at $\theta_0 = 0^0$ is for any wave size C close to the angular characteristic $D(\theta)$ of the hard spheroid.

Figure 1-7 shows sections σ_0 of prolate spheroidal scatterers. The steel prolate spheroid is irradiated by the sound wave at an angle of $\theta_0 = 90^0$ has the resonance of the surface wave with the same meaning $C =$ 7,4 (see curve 2, Fig. 1-5) [1]. The same section of the scattering σ_0 of the steel continuous spheroid (curve 3), which is irradiated by the sound wave at an angle of $\theta_0 = 90^0$, is visibly closer to the σ_0 of the hard spheroid (curve 4) in comparison with the σ_0 of the soft spheroid (curve 5). This similarity in the scattering properties of continuous elastic and hard spheroids was also shown in the angular characteristic $D(\theta, \varphi)$. The frequency dependence of the relative section σ_0 in the prolate spheroidal shell (curve 1) irradiated by the sound wave at an angle of $\theta_0 = 0^0$ shows the presence of considerable resonance by $C = 6,75$ [1, 2, 8, 9]. Figure 1-8 shows the modular uses of angular characteristics $|D(\theta)|$ in prolate spheroidal scatterers. Curve 1 is the steel, gas-filled shell with a wave dimension $C = 6,75$ that corresponds to its resonance. Curve 2 is a soft spheroid, while curve 3 is a hard spheroid. For all ideal spheroids, the wave size C is equal to 10,0. From the comparison of the three curves, we can see that the shaded lobe of shell's angular characteristic is shown as the "soft background", but the lobe of the backscattering is shown as the "hard background".

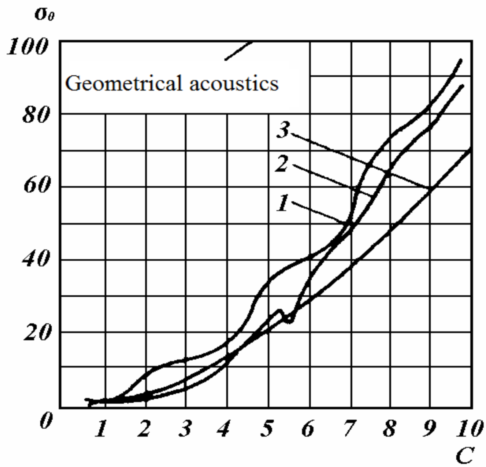

Figure 1-6: The relative backscattering in the cross-sections of oblate spheroid

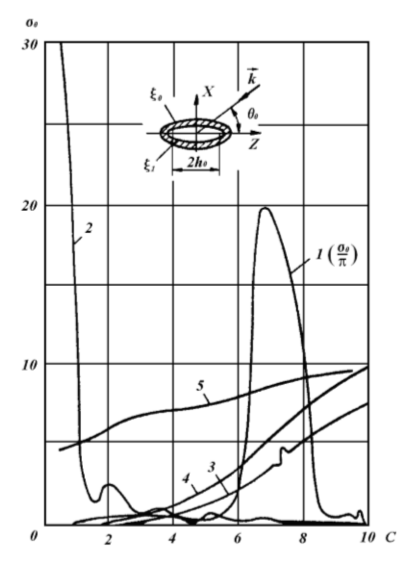

Figure 1-7: The relative backscattering in cross-sections of the prolate spheroidal scatterer

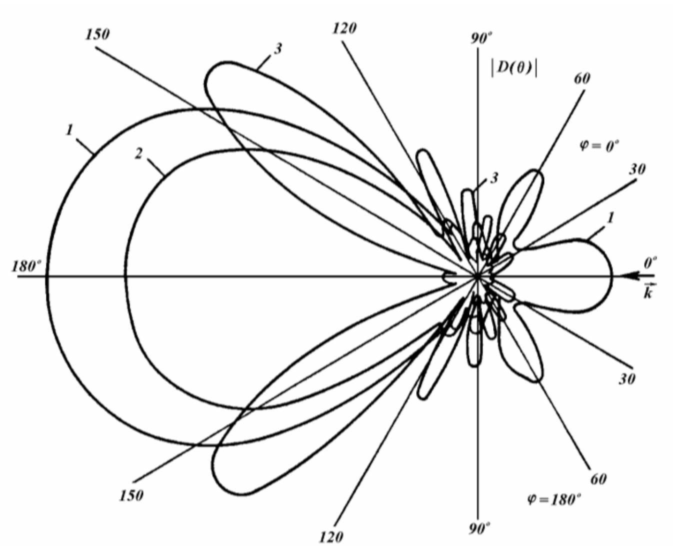

Figure 1-8: Modules with the angular characteristics of prolate spheroidal bodies

Table 1-1

Wave size C	σ_0 at an angle of $\theta_0 = 90^\circ$		
	Spheroidal gas-filled shell $\xi_0 = 1{,}005075;$ $\xi_1 = 1{,}005$	Hard spheroid $\xi_0 = 1{,}005$	Soft spheroid $\xi_0 = 1{,}005$
0,5	$0{,}3012 \cdot 10^{-3}$	$0{,}2452 \cdot 10^{-3}$	4,506
1,0	$0{,}4748 \cdot 10^{-2}$	$0{,}3908 \cdot 10^{-2}$	4,760
1,5	$0{,}2365 \cdot 10^{-1}$	$0{,}1965 \cdot 10^{-1}$	5,194
2,0	$0{,}7354 \cdot 10^{-1}$	$0{,}6147 \cdot 10^{-1}$	5,748
2,5	0,1751	0,1479	6,300
3,0	0,3470	0,3006	6,754
3,5	0,6068	0,5418	7,094
4,0	0,9736	0,8911	7,358
4,5	1,447	1,362	7,592
5,0	2,014	1,960	7,815

The relative backscattering of the cross-section σ_0 of a spheroidal shell irradiated by a sound wave at an angle of $\theta_0 = 90^0$ was calculated for a wave size ranging from C=0,5 to $C = 5{,}5$. The meanings of the σ_0 in a shell are very similar to the σ_0 in a hard spheroid; it is worthwhile to compare these sections in tabular form. As it can be seen from Table 1-1, the angle of the shell's irradiation with wave sizes ranging from C=0,5 to $C = 5{,}5$ indicates a "hard background" to the scattering. This is what we can see from a comparison of the angular characteristics of the scattering $D(\theta, \varphi)$.

1.2. Characteristics of Anisotropic Spheroidal Scatterers

Let us pay attention to an anisotropic (transversal-isotropic) spheroidal scatterer. A transversely-isotropic medium is characterized by five elastic moduli: $A_{11}, A_{12}, A_{13}, A_{33}, A_{44}$. Hooce's generalized law for such a body is presented in the form [18, 19]:

$$\left.\begin{aligned}
\sigma_\eta &= A_{11}\varepsilon_\eta + A_{12}\varepsilon_\varphi + A_{13}\varepsilon_\xi;\\
\sigma_\varphi &= A_{12}\varepsilon_\eta + A_{11}\varepsilon_\varphi + A_{13}\varepsilon_\xi;\\
\sigma_\xi &= A_{13}\left(\varepsilon_\eta + \varepsilon_\varphi\right) + A_{33}\varepsilon_\xi;\\
\tau_{\eta\varphi} &= A_{44}\gamma_{\eta\varphi};\\
\tau_{\xi\varphi} &= A_{44}\gamma_{\xi\varphi};\\
\tau_{\eta\varphi} &= \frac{1}{2}\left(A_{11} - A_{12}\right)\gamma_{\eta\varphi},
\end{aligned}\right\}$$

where: $\sigma_\xi, \sigma_\eta, \sigma_\varphi, \tau_{\xi\eta}, \tau_{\xi\varphi}, \tau_{\eta\varphi}$ - are the components of the stress tensor, $\varepsilon_\xi, \varepsilon_\eta, \varepsilon_\varphi, \gamma_{\xi\eta}, \gamma_{\xi\varphi}, \gamma_{\eta\varphi}$ - are components of deformation, which, in turn, are equal in spheroidal coordinates:

$$\varepsilon_\xi = (h_\xi)^{-1} \bullet \frac{\partial u_\xi}{\partial \xi} + (h_\xi h_\eta)^{-1} \bullet \frac{\partial h_\xi}{\partial \eta} \bullet u_\eta; \varepsilon_\eta = (h_\eta)^{-1} \bullet \frac{\partial u_\eta}{\partial \eta} + (h_\eta h_\xi)^{-1} \bullet \frac{\partial h_\eta}{\partial \xi} \bullet u_\xi;$$

$$\varepsilon_\varphi = (h_\varphi)^{-1} \bullet \frac{\partial u_\varphi}{\partial \varphi} + (h_\xi h_\varphi)^{-1} \bullet \frac{\partial h_\varphi}{\partial \xi} \bullet u_\xi + (h_\eta h_\varphi)^{-1} \bullet \frac{\partial h_\varphi}{\partial \eta} \bullet u_\eta;$$

$$\gamma_{\xi\eta} = (h_\xi)^{-1} h_\eta \bullet \frac{\partial}{\partial \xi}\left(\frac{u_\eta}{h_\eta}\right) + (h_\eta)^{-1} h_\xi \bullet \frac{\partial}{\partial \eta}\left(\frac{u_\xi}{h_\xi}\right);$$

$$\gamma_{\xi\varphi} = (h_\xi)^{-1} h_\varphi \bullet \frac{\partial}{\partial \xi}\left(\frac{u_\varphi}{h_\varphi}\right) + (h_\varphi)^{-1} h_\xi \bullet \frac{\partial}{\partial \varphi}\left(\frac{u_\xi}{h_\xi}\right);$$

$$\gamma_{\eta\varphi} = (h_\eta)^{-1} h_\varphi \bullet \frac{\partial}{\partial \eta}\left(\frac{u_\varphi}{h_\varphi}\right) + (h_\varphi)^{-1} h_\eta \bullet \frac{\partial}{\partial \varphi}\left(\frac{u_\eta}{h_\eta}\right);$$

There are two orientations of such an anisotropic spheroidal scatterer for which the characteristics of an isotropic spheroidal body, in this case, the elastic moduli in the plane of isotropy of transversely isotropic scatterer will coincide with the elastic moduli of isotropic body.

1) angle of incidence $\theta_0 = 90^\circ$, viewing angle θ is also 90°, and the planes of isotropy angle of incidence $\theta_0 = 90^\circ$, viewing angle θ is also 90°, and the planes of isotropy of the anisotropic spheroidal scatterer are perpendicular to the axis of rotation Z (see Fig. 1-1), thus curve 3 of Figure 1-7, depicting the relative backscattering in the cross-sections σ_0 will be common for a prolate steel spheroid and the corresponding transversely isotropic spheroid;
2) at an angle $\theta_0 = 0^\circ$ (axisymmetric problem), the planes of isotropy of an anisotropic body correspond to the condition $\varphi = const$ and contain the axis of rotation Z. Curves with number 2 in Figures 1-5 and 1-6, characterizing the dispersion σ_0 of steel spheroids, will coincide with the corresponding anisotropic scatterers. Curve 1 refers to a steel gas-filled shell and at the selected irradiation angle $\theta_0 = 0^\circ$ will have an anisotropic analogue with the same characteristic. An analogue coincidence Awill be observed for the modulus of the angular scattering characteristic $|D(\theta)|$ (curve 1 of Fig. 1-8, $\theta_0 = 0^\circ$). Axes 1 and 2 lie in the plane of isotropy, and axis 3 is perpendicular to this plane (for both orientation).

1.3. Characteristics of Anisotropic Cylindrical Scatterers

Let us turn to the problem of diffraction of elastic waves by a transversely isotropic infinite cylinder placed in an isotropic medium [20]. The geometry of the problem is presented in the Figure 1-9. The displacement vector $\vec{u}$ is represented as:

$$\vec{u} = grad\,\Phi + rot\,\vec{A}. \tag{1.25}$$

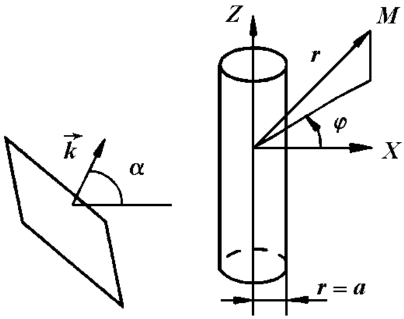

Figure 1-9: The transversely isotropic plane wave irradiated cylinder

For the vector function $\vec{A}$, in turn, the decomposition was proposed in [20]:

$$\vec{A} = \chi \vec{e}_z + a \cdot rot(\psi \vec{e}_z), \tag{1.26}$$

where: χ and ψ are scalar functions obeying the scalar Helmholtz equation, $\vec{e}_z$ - Z –is axis unit vector, a –is cylinder radius.

Potentials Φ_i and χ_i (polarization r-φ) and ψ_i (polarization r-z) are presented in the form of expansions in cylindrical functions:

$$\Phi_i = \sum_{n=0}^{\infty} \in_n (i)^n J_n(k_{1\perp} r) cos(n\varphi) exp[k_{1z} z - \omega t], \tag{1.27}$$

where: $k_{1\perp} = k_1 cos\alpha$, $k_{1z} = k_1 sin\alpha$, k_1 - is longitudinal wavenumber in the cylinder material;

$$\chi_i = \sum_{n=1}^{\infty} \in_n (i)^n J_n(k_{2\perp} r) sin(n\varphi) exp[i(k_{2z} z - \omega t)], \tag{1.28}$$

where: $k_{2\perp} = k_2 cos\alpha$, $k_{2z} = k_2 sin\alpha$, k_2 - is the wavenumber of a shear wave in a cylinder material;

$$\psi_i = \sum_{n=0}^{\infty} \in_n (i)^n J_n(k_{2\perp} r) cos(n\varphi) exp[i(k_{2z} z - \omega t)], \tag{1.29}$$

Potentials Φ, Ψ and χ of the transversely isotropic cylinder itself are determined by the expansions [20]:

$$\Phi_1 = \sum_{n=0}^{\infty}\left[A_n J_n(s_1 r) + q_2 B_n J_n(s_2 r)\right]cos(n\varphi)exp\left[i(k_z z - \omega t)\right]; \quad (1.30)$$

$$\psi_1 = \sum_{n=0}^{\infty}\left[q_1 A_n J_n(s_1 r) + B_n J_n(s_2 r)\right]cos(n\varphi)exp\left[i(k_z z - \omega t)\right]; \quad (1.31)$$

$$\chi_1 = \sum_{n=1}^{\infty} C_n J_n(s_3 r) sin(n\varphi) exp\left[i(k_z z - \omega t)\right], \quad (1.32)$$

where: A_n, B_n, C_n - unknown expansion coefficients determined by from boundary conditions; $k_z = k_{1z}$ - in the case of a longitudinal wave incidence on the cylinder; $k_z = k_{2z}$ - for the incident shear wave;

$$s_1^2 = \frac{\xi - \sqrt{\xi^2 - 4\varsigma A_{11} A_{44}}}{2A_{11}A_{44}};$$

$$s_2^2 = \frac{\xi + \sqrt{\xi^2 - 4\varsigma A_{11} A_{44}}}{2A_{11}A_{44}};$$

$$s_3^2 = \frac{2(\rho_1 \omega^2 - A_{44} k_z^2)}{A_{11} - A_{12}};$$

$$\xi = (A_{13} + A_{44})^2 k_z^2 + A_{11}(\rho_1 \omega^2 - A_{33} k_z^2) + A_{44}(\rho_1 \omega^2 - A_{44} k_z^2);$$

$$\varsigma = (\rho_1 \omega^2 - A_{44} k_z^2)(\rho_1 \omega^2 - A_{33} k_z^2);$$

ρ_1 - cylinder material density.

Potentials Φ_s, ψ_s and χ_s of scattered waves in an isotropic medium are presented in the forms of expansions:

$$\Phi_s = \sum_{n=0}^{\infty} D_n H_n^{(1)}(k_{1\perp} r) cos(n\varphi) exp\left[i(k_z z - \omega t)\right]; \quad (1.33)$$

$$\Psi_s = \sum_{n=0}^{\infty} E_n H_n^{(1)}(k_{2\perp} r) cos(n\varphi) exp[i(k_z z - \omega t)] ; \tag{1.34}$$

$$\chi_s = \sum_{n=1}^{\infty} F_n H_n^{(1)}(k_{2\perp} r) sin(n\varphi) exp[i(k_z z - \omega t)] , \tag{1.35}$$

where: D_n, E_n, F_n are unknown expansion coefficients determined by boundary conditions.

The displacement vector $\vec{u}$ in isotropic medium consists of two components:

$$\vec{u} = \vec{u}_i + \vec{u}_s \ . \tag{1.35}$$

Boundary conditions on the surface of the cylinder consist in the continuity of three components of the displacement vector and three components of the stress tensor (normal and two tangential), this leads, when finding the unknown D_n, E_n and F_n of the scattered waves according to Cramer's rule, to the ratio of the determinants of the 6th order. Figures 1-10 and 1-11 show the normalized back reflection amplitudes for transversely isotropic cylinders. Figure 1-10 shows the form-function of the back reflection of an axially polarized shear wave resulting from irradiation of a cylinder with a radius *a =0,37* mm by an axially polarized shear wave at an angle $\alpha = 0^{\circ}$.

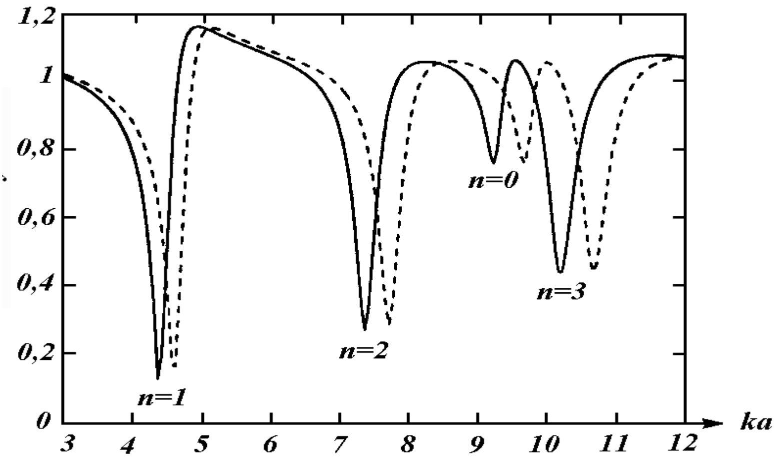

Figure 1-10: The form-function of the back reflection

Figure 1-10 corresponds to an isotropic stainless - steel cylinder, the dotted line – to a steel cylinder, in which elastic

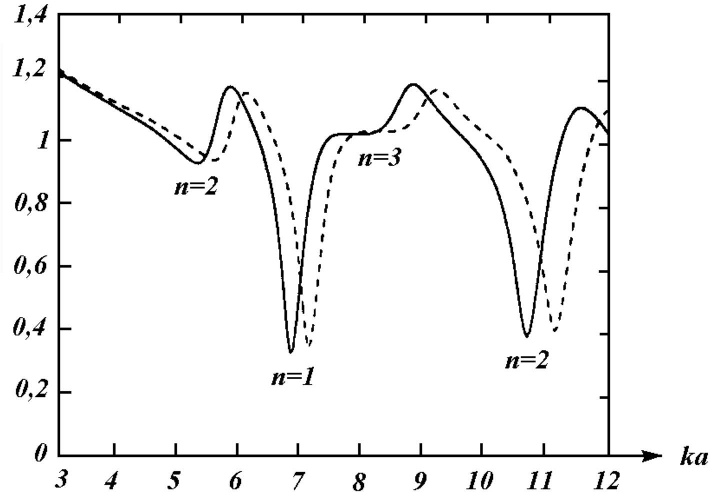

Figure 1-11: The form-function of the back reflection

The cylinder is embedded in an isotropic epoxy matrix. The solid line in moduli have increased by 10% A_{44} and A_{55}, wherein $A_{44} = A_{55}$. Other modules have not changed.

Figure 1-11 shows the form-function of the back reflection of a shear wave polarized in the plane *r-φ*, resulting from irradiation of the cylinder at an angle $\alpha = 0^{\circ}$. The cylinder is enclosed in an isotropic epoxy matrix. The solid line is an isotropic stainless - steel cylinder, the dashed line is the same cylinder which module A_{66} is increased by *10%*. the value of the module A_{11}, has been adjusted accordingly, since $A_{11} = A_{66}$.

1.4. Plane Waveguide with Anisotropic Bottom

It is well known [21] that a pulsed sound signal, like a bunch of energy, propagates at a group velocity. This circumstance forces us to use the method of imaginary sources when studying the temporal characteristics of pulsed signals scattered by various bodies placed in a plane waveguide [22

– 27]. Wherein the spectral characteristics of the pulses dea-ling with continuous harmonic signals can be also studied using the normal wave method [28].

When studying waves in anisotropic media, the initial equations are the dynamic equilibrium of continuous medium [18, 19, 29 – 31]:

$$\left.\begin{aligned}\frac{\partial\sigma_x}{\partial x}+\frac{\partial\tau_{yx}}{\partial y}+\frac{\partial\tau_{zx}}{\partial z}=\rho\frac{\partial^2 u}{\partial t^2};\\ \frac{\partial\sigma_y}{\partial y}+\frac{\partial\tau_{xy}}{\partial x}+\frac{\partial\tau_{zy}}{\partial z}=\rho\frac{\partial^2 \upsilon}{\partial t^2};\\ \frac{\partial\sigma_z}{\partial z}+\frac{\partial\tau_{xz}}{\partial x}+\frac{\partial\tau_{yz}}{\partial y}=\rho\frac{\partial^2 w}{\partial t^2},\end{aligned}\right\} \tag{1.37}$$

We restrict ourselves to the consideration of plane monochromatic waves [31], the general expression of the displacement vector of such a wave can be written as:

$$\vec{u}=\vec{u}^{0}\cdot e^{i\left(\vec{k}\,\vec{r}-\omega t\right)}, \tag{1.38}$$

where: $\vec{u}^{0}$ - is the constant vector (independent of either coordinates or time), called the vector amplitude of the wave.

The displacement vector (1.38) will only in that case will satisfy the equations of motion (1.37) if its real and imaginary parts individually satisfy the same equation. If the vector amplitude $\vec{u}^{\circ}$ is real, then:

$$\vec{u}=\vec{u}^{\circ}\left(cos\varphi+i\,sin\,\varphi\right)=\vec{u}'+i\,\vec{u}'', \tag{1.39}$$

moreover $\vec{u}'=\vec{u}^{\circ}\cdot cos\left(\vec{k}\,\vec{r}-\omega t\right)$ and $\vec{u}''=\vec{u}^{\circ}\cdot sin\left(\vec{k}\,\vec{r}-\omega t\right)$ are real solutions of the basic equations (1.37) in the form of plane monochromatic waves. Therefore, we can always choose any of them, for example, $\vec{u}'$, as a real solution. A plane monochromatic wave (1.38) will not satisfy the equations of motion (1.37) for any parameter values $\vec{u}^{\circ},\vec{k},\omega$. We rewrite the equations of motion (1.37) in another form, using the notation of the elastic moduli as components of the 4th rank tensor [25]:

$$\rho \frac{\partial^2 u_i}{\partial t^2} = c_{ijlm} \frac{\partial^2 u_m}{\partial x_j \partial x_l} \tag{1.40}$$

$(i, j, l, m = 1,2,3)$

Substituting (1.38) in (1.40) and considering that $\frac{\partial}{\partial x_j} e^{i\vec{k}\vec{r}} = \frac{\partial}{\partial x_j} e^{ik_l x_l} = i k_j e^{i\vec{k}\vec{r}}$, we obtain:

$$\rho \omega^2 u_i = c_{ijlm} k_j k_l u_m \tag{1.41}$$

We introduce instead c_{ijlm} of the tensor

$$\lambda_{ijlm} = \frac{1}{\rho} c_{ijlm} , \tag{1.42}$$

which we will call the reduced tensor of elastic moduli.

Considering that $\vec{k} = k\vec{n}$ ($\vec{n}$ is the unit vector); $\vec{n}^2 = 1;\ k = |\vec{k}|;$ $k_j = k n_j ;\ c = \omega/k$, we rewrite (1.42) in the form:

$$\lambda_{ijlm} n_j n_l u_m - c^2 u_i = 0 \tag{1.43}$$

If we introduce a tensor of the second rank:

$$\Lambda = \Lambda^{\vec{n}} = (\Lambda_{im}) = (\lambda_{ijlm} n_j n_l), \tag{1.44}$$

then equation (1.43) can be written in direct form:

$$(\Lambda - \lambda)\vec{u} = 0, \tag{1.45}$$

From (1.45) it follows that the displacement vector of plane wave $\vec{u}$ is an eigenvector, and the square of the phase velocity of the wave c^2 is an eigenvalue of the tensor Λ.

Vector equation (1.45) is the main one for the theory of elastic waves in anisotropic media and is called the Christoffel equation. Solving this equation is reduced to finding the eigenvectors and eigenvalues of the tensor Λ.

A real symmetric positive definite (for any directions of the wave normal) tensor Λ in the general case has three different eigenvalues $\lambda_1 = c_1^2\,;\lambda_2 = c_2^2\,;\lambda_3 = c_3^2$, each of which has its own vector that determines the direction of displacement in the wave. Therefore, three waves with different phase velocities can propagate in anisotropic media in the general case, for any given direction of the wave normal. We will call such three waves, having a common wave normal, isonormal.

Transversely isotropic elastic medium is characterized by five elastic modules: $A_{11}, A_{12}, A_{13}, A_{33}, A_{44}$, and the generalized Hooke's law for such a medium is written in the form [18, 19, 29 - 31]:

$$\left.\begin{aligned}
\sigma_y &= A_{11}\,\varepsilon_y + A_{12}\,\varepsilon_z + A_{13}\,\varepsilon_x\,;\\
\sigma_z &= A_{12}\,\varepsilon_y + A_{11}\,\varepsilon_z + A_{13}\,\varepsilon_x\,;\\
\sigma_x &= A_{13}\left(\varepsilon_y + \varepsilon_z\right) + A_{33}\,\varepsilon_x\,;\\
\tau_{yx} &= A_{44}\,\gamma_{yx}\,;\\
\tau_{zx} &= A_{44}\,\gamma_{zx}\,;\\
\tau_{yz} &= \frac{1}{2}(A_{11} - A_{12})\gamma_{yz}\;,
\end{aligned}\right\} \tag{1.46}$$

where: $\varepsilon_y, \varepsilon_z, \varepsilon_x, \gamma_{yx}, \gamma_{yz}, \gamma_{zx}$ are deformation components.

The problem will be solved in a flat setting, i. e. the displacement vector $\vec{U}$ has only two components other than zero U (on the X axis) and W (on the Z axis) and there is no dependence on the coordinate y. Taking this into account, the deformation components will be equal to:

$$\left.\begin{aligned}
&\varepsilon_x = \frac{\partial U}{\partial x}; \quad \varepsilon_y \equiv 0; \quad \varepsilon_z = \frac{\partial W}{\partial z};\\
&\gamma_{yx} \equiv 0; \quad \gamma_{yz} \equiv 0; \quad \gamma_{zx} = \frac{\partial U}{\partial z} + \frac{\partial W}{\partial x},
\end{aligned}\right\} \tag{1.47}$$

And Hooke's law will be simplified:

$$\left.\begin{aligned}
\sigma_y &= A_{12}\,\varepsilon_z + A_{13}\,\varepsilon_x = A_{12}\frac{\partial W}{\partial z} + A_{13}\frac{\partial U}{\partial x};\\
\sigma_z &= A_{11}\,\varepsilon_z + A_{13}\,\varepsilon_x = A_{11}\frac{\partial W}{\partial z} + A_{13}\frac{\partial U}{\partial x};\\
\sigma_x &= A_{13}\,\varepsilon_z + A_{33}\,\varepsilon_x = A_{13}\frac{\partial W}{\partial z} + A_{33}\frac{\partial U}{\partial x};\\
\tau_{zx} &= A_{44}\,\gamma_{zx} = A_{44}\left(\frac{\partial U}{\partial z} + \frac{\partial W}{\partial x}\right)
\end{aligned}\right\} \tag{1.48}$$

The equations of dynamic equilibrium for a flat formulation take the form:

$$\left.\begin{aligned}
\frac{\partial \sigma_x}{\partial x} + \frac{\partial \tau_{zx}}{\partial z} + \rho_1\,\omega^2 U = 0;\\
\frac{\partial \tau_{zx}}{\partial x} + \frac{\partial \sigma_z}{\partial z} + \rho_1\,\omega^2 W = 0,
\end{aligned}\right\} \tag{1.49}$$

where: ρ_1 – is transverse isotropic half – space density.

We turn to a familiar problem of the diffraction of pulses on spheroidal bodies in the plane waveguide [19, 29, 30], retaining the upper boundary condition of Dirichlet, waveguide dimensions and scatterer with respect to boundaries, replacing only ideal hard boundary on the elastic isotropic bottom. Physical parameters of the lower medium will correspond to the isotropic elastic bottom, but in their values, they will be very close to parameters of transversely-isotropic rock – a large gray siltstone [18]. The longitudinal wave velocity in this material is 4750 m/s, the transverse wave velocity – 2811m/s. When used in this case the method of imaginary sources, we need to enter the reflection coefficient *V* for each source [32], when displaying sources are relative to the upper border sources, as before [1, 18, 19, 27, 28, 29, 30, 32], we will change the sign on the opposite, this corresponds to a change of phase by π .

It is known to [32], that the imaginary sources method boundary conditions are not fulfilled strictly on any of borders of the waveguide even in the case of ideal boundary conditions of Dirichlet and Neumann. For the better